




AKADÉMIAI KIADÓ

# Lateral-torsional buckling resistance of corrugated web girders

Erzsébet Bärnkopf<sup>1\*</sup> , Bence Jáger<sup>2</sup> and Balázs Kövesdi<sup>2</sup>

Pollack Periodica •  
An International Journal  
for Engineering and  
Information Sciences

<sup>1</sup> Pál Vásárhelyi Doctoral School of Civil Engineering and Earth Sciences, Faculty of Civil Engineering, Budapest University of Technology and Economics, Budapest, Hungary

<sup>2</sup> Department of Structural Engineering, Faculty of Civil Engineering, Budapest University of Technology and Economics, Budapest, Hungary

Received: December 29, 2022 • Revised manuscript received: April 13, 2023 • Accepted: April 17, 2023

DOI:

10.1556/606.2023.00797

© 2023 The Author(s)

ORIGINAL RESEARCH  
PAPER



## ABSTRACT

There is currently no accurate calculation procedure for determining the lateral-torsional buckling resistance of trapezoidally corrugated web girders. Therefore, a detailed investigation is performed in the frame of an experimental and numerical research program at the Department of Structural Engineering of the Budapest University of Technology and Economics. Based on the previous experimental results, a numerical model is developed to be used to determine the lateral-torsional buckling resistance by using deterministic method. The effect of flange size, corrugation geometry and boundary conditions are investigated. An improved design method is developed for the determination of the lateral-torsional buckling resistance of trapezoidally corrugated web girders.

## KEYWORDS

lateral-torsional buckling, corrugated web, trapezoidally corrugation, finite element analysis

## 1. INTRODUCTION

The web of the traditional steel beam is flat, requiring stiffeners both transversely and longitudinally. These stiffeners are post-welded to the thin web panels to prevent local or global buckling, which procedure is labor intensive. The innovation of the trapezoidally corrugated girders is that the flat web plate is replaced by a corrugated web, thus reducing the amount of work by avoiding post-welding. In addition, the web can generally be thinner in this case, so that overall lighter structures can typically be built. The only major difficulty with this type of girder is that special technology is required to manufacture trapezoidally corrugated web girders.

The use of trapezoidally corrugated beams began in Sweden, where these structures were already in use in the late 1960s [1]. Today, they are mainly used in industrial and commercial buildings and in bridge construction, where their high load-bearing capacity compared to the use of materials is particularly advantageous. Trapezoidally corrugated web girders have spread relatively quickly and are becoming increasingly popular in the structural engineering practice. Numerous bridges with corrugated web have been built in the world, also in Hungary (M43 Tisza-bridge and the new Paks-Kalocsa Danube bridge is currently being built also with trapezoidally corrugated web girders).

The previous research results show these structures differ from conventional I-beams in their lateral-torsional buckling behavior. In a similar way, differences in structural behavior were observed in this case, as Bartuš and Odrobiňák [2] showed for another girder that the occurrence of strap openings affects the lateral-torsional stability of the girders. Therefore, their design, and the Lateral-Torsional Buckling (LTB) resistance calculation method require detailed investigations. The first studies are attributed to Lindner [1], who investigated the elastic critical moment of trapezoidally corrugated girders, and then, taking into account

\*Corresponding author.

E-mail: [bamkopf.erzsebet@edu.bme.hu](mailto:bamkopf.erzsebet@edu.bme.hu)

 AKJournals

the initial imperfections, their LTB resistance was also investigated. He observed that these values are significantly higher than those of their conventional flat web competitors. Following the results of Lindner, numerous researchers confirmed his claim.

Lindner [1] has refined the equation elastic critical moment in the case of a beam using traditional flat web subjected to a constant bending moment for the case of trapezoidally corrugated girders by adding an extra term to the warping constant in the formula. In this way, the higher performance experienced is taken into account. This term was given a correction factor  $c_w$  and included length, even though the  $I_w$  warping constant should be theoretically a cross-sectional property.

In 2013, Larsson and Persson [3] performed an extensive numerical study and confirmed the equation suggested by Lindner. In this study, Larsson and Persson modified the equation, which had theoretical significance. Namely, the two formulas result practically equal elastic critical moments, but with the revision, all cross-sectional properties are independent of the span length. In 2013, Ilanovský [4] also confirmed that the elastic critical moment and ultimate strength of trapezoidally corrugated beams are higher than those of conventional flat web beams.

Following the proposal of Larsson and Persson, in 2017 Lopes et al. [5] tested trapezoidally and sinusoidal corrugated web girders too. Based on a comprehensive numerical research program they modified the values of the parameters  $c_1$  and  $c_2$  in the formula.

So far, no general design procedure has been developed to calculate the LTB resistance of trapezoidally corrugated web girders. Only suggestions for the determination of the elastic critical moment have been given. Hence, further investigations are needed to better understand their structural behavior and to determine the critical load parameter and the reduction factor associated with the LTB.

## 2. RESEARCH STRATEGY AND NUMERICAL MODELING

### 2.1. Research strategy

The main purpose of this study is twofold. On the one hand, they aim to define an equivalent imperfection, which could be used in Geometric and Material Nonlinear Imperfection Analysis (GMNIA). Equivalent geometric imperfections are sought, related to the manufacturing tolerances of EN 1090-2:2018 [6], both shape and size specifications are required. On the other hand, the second objective is to determine which buckling curve from EN 1993-1-1:2005 [7] can be applied to determine the LTB resistance of trapezoidally corrugated web girders. Imperfections are of primary importance in determining resistance. Therefore, special attention should be paid to this issue and the imperfections should be investigated by treating them together as initial geometric imperfections and residual stresses, and also their equivalent geometric imperfections should be determined, and the results compared.

Two kinds of analysis are performed on the Finite Element (FE) model: the elastic critical moment is determined from Linear Buckling Analysis (LBA) the lateral-torsional buckling resistance is calculated using GMNIA. The results are statistically evaluated according to EN 1990:2002 [8] and the required resistance-side partial factor is determined for each buckling curve from EN 1993-1-1:2005 [7].

### 2.2. Numerical model development and validation

An advanced FE model is developed using ANSYS 19.2 software [9]. The model is verified, a detailed mesh-sensitivity test is carried out, and it is validated by using the results of a laboratory test performed at the Department of Structural Engineering of Budapest University of Technology and Economics (BUTE) in 2018 [10]. In the experiments, eleven real-size test specimens were examined by four-point-bending. Six types of cross-section geometry (the difference was in the flange size) were investigated but the corrugation profile was not varying. The primary objective of the series of laboratory experiments was to determine the imperfections of the fabricated girders and their LTB resistance. The model development and the details of the validation are presented in [10].

In the parametric study simply supported girder subjected by constant bending moments is studied, which is the basic case for the LTB buckling curve development. The FE model uses four-node shell elements, namely Shell 181 in the software. Figure 1 shows the meshed numerical model; together with the boundary conditions and the force couple

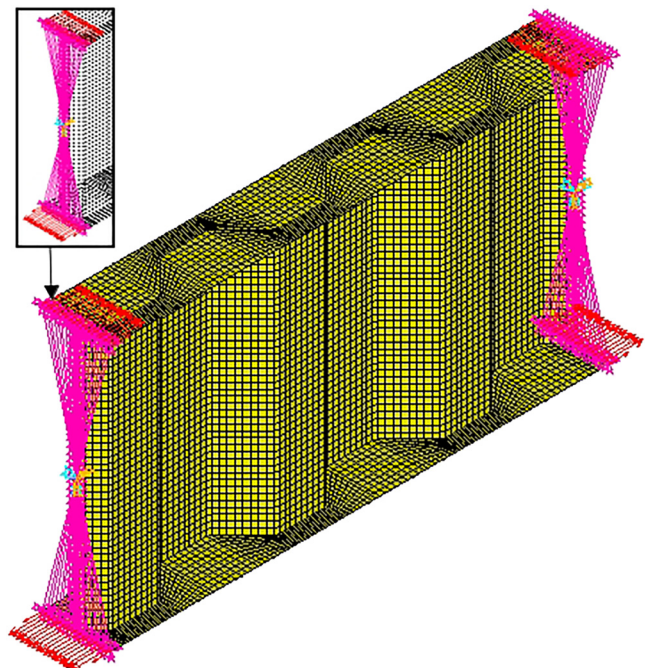


Fig. 1. The meshed FE model (illustrating both the boundary conditions and the applied load shortest span)  
(Source: Authors' result)

(distributed along the width of the flange) resulting in the bending moment shown by arrows.

The model provides a choice of free or fixed warping and rotation about the vertical axis at the ends. Based on Timoshenko [11] and EN1993-1-1 [7], this effect is taken into account in Eq. (1) by the factors  $k_w$  and  $k$  for the case of the beam using traditional flat web subjected to a constant bending moment,

$$M_{cr} = \frac{\pi}{k \cdot L} \sqrt{EI_Z \left[ \left( \frac{\pi}{k_w \cdot L} \right)^2 EI_w + GI_t \right]}, \quad (1)$$

where  $M_{cr}$  is the elastic critical moment;  $E$  is the elastic modulus;  $G$  is the shear modulus;  $k$  is the effective length factor about the weak axis rotation;  $L$  is the span length of the girder;  $I_Z$  is the moment of inertia about the minor axis;  $k_w$  is the effective length factor with respect to warping;  $I_w$  is the warping constant;  $I_t$  is the torsional constant.

With the factors  $k_w$  and  $k$ , the three boundary conditions can be easily described first when both warping and rotation are free ( $k_w = k = 1.0$ ), rotation is free, but warping is fixed ( $k_w = 0.5$  and  $k = 1.0$ ), and both are fixed ( $k_w = k = 0.5$ ). In the model, a master node is created, to which the end cross-section nodes are connected by assigning the relevant degrees of freedom, thus producing different layouts.

In the first case, only the transverse and vertical displacements and the twist around the longitudinal axis are blocked. In the second case, the longitudinal displacement of the nodes of the end cross-section is blocked in addition to these. In the third case, both the longitudinal displacement and the twist around the vertical axis are fixed.

The material model used in GMNIA is the multi-linear model, which is proposed by Gardner et al. [12]. Only steel S355 (using  $f_y = 355$  MPa as yield strength,  $f_u = 510$  MPa as tensile strength, and  $E = 210$  GPa as elastic modulus) is tested. Two approaches are existing to determine LTB resistance:

- i) reduction factor procedures (traditional); and
- ii) numerical model-based design procedures using substitution imperfection.

In the last decades, the former approach has been mainly used, in which the reduction factor is determined based on buckling curves. Therefore, the development of empirical buckling curves was previously essential for the design praxis, although they have also a strong theoretical background. In the practice, buckling curves are usually based on the statistical evaluation of a large dataset of experimental results. In the past, experiments could only be laboratory tests. Nowadays they can be replaced by numerical simulations, where imperfections are directly taken into account in the FE model and the LTB resistance is calculated by geometrically and materially nonlinear analysis. The use of numerical simulations allows a large number of virtual tests to be carried out, allowing a highly accurate statistical evaluation to be made. The second approach is the numerical model-based design approach using substitution imperfection, which makes it possible to determine the LTB

resistance by the numerical model directly, without using the buckling curves. Using this design method, highly accurate and reliable equivalent geometric imperfections should be developed.

In this paper, both approaches are addressed; first the determination of the required equivalent geometric imperfections is presented in the context of the numerical model-based design procedure.

## 3. RESULTS AND DISCUSSION

### 3.1. Equivalent geometric imperfection calibration

In the imperfection-sensitivity analysis, five cross-sections are tested, which only differ in their flange width, thickness, and corrugation angle. For each specimen, the height of the web ( $h_w$ ) is 520 mm, and its thickness ( $t_w$ ) is 6 mm. Each cross-section is doubly symmetrical; the five different sizes of flanges are summarized in Table 1.

The applied trapezoidally corrugation profile does not change during the tests and is characterized by the following parameters:  $\alpha = 45^\circ$ ,  $a_1 = a_2 = 98$  mm; see Fig. 2 for markings.

The different corrugation angles only in case of a) flange size are investigated (see Table 1), applying  $\alpha = 30^\circ$  and  $40^\circ$  (other parameters of the model remain unchanged). In total 6 to 8 different slenderness are tested using different spans. In the imperfection-sensitivity study, the first global buckling eigenmode is determined from LBA and applied as an artificial geometric imperfection with the corresponding scaling. Local imperfections have been neglected in the modeling, since the applied flanges were not sensitive for local buckling (no class 4 flanges were studied) and according to Jáger [13] the effect of the flange imperfection for this particular case is less than 1–2%.

The equivalent geometric imperfection, which is required, is obtained to have the same effect on the numerical model-based resistance as the initial geometric imperfection of  $L/1000$  magnitude together with the expected residual stresses. The magnitude, namely  $L/1000$  is

Table 1. The investigated flange sizes using the notations of Fig. 2

	$b_f$ [mm]	$t_f$ [mm]
a)	140	14
b)	160	14
c)	180	14
d)	220	16
e)	250	16

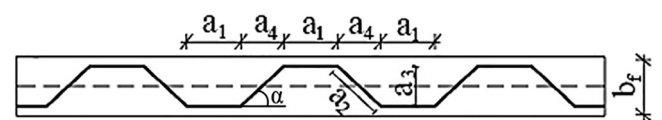


Fig. 2. Applied notations related to the corrugation profile (Source: Authors' plot)



defined in Annex B of EN 1090-2:2018 [6] it means the greatest tolerated value for member out-of-straightness. The used residual stress pattern is derived from [10], which pattern has an experimental-based origin.

In the imperfection-sensitivity study, the load-carrying capacity is determined using several different equivalent geometric imperfection magnitudes for every different girder type. The first global buckling eigen-mode is determined from LBA and applied as an artificial geometric imperfection with the corresponding scaling. The maximum displacement value in the middle of the girder was always  $L/xxx$ . In this calculation, the required values of equivalent geometric imperfection magnitudes ( $xxx$ ) are obtained from linear interpolation. Figure 3 shows the final results of the investigation. On the diagram the vertical axis indicates the so-called scaling factor on the span length  $L$  and the horizontal axis represents the relative slenderness ratio of the corrugated web girder regarding lateral torsional buckling (by calculating the critical bending moment using the numerical model for the relative slenderness ratio).

The effect of equivalent geometric imperfections shown in Fig. 3 is equal to the effect of initial geometric imperfections combined with residual stresses. The tendency of the curves is the same for all flange sizes tested. The wider the flanges the larger the scaling factor of  $L$ , so the smaller the magnitude of equivalent geometric imperfection. If the relative slenderness is less than 0.7 then the differences between the curves are greatly reduced, whereas for larger relative slenderness the differences are significant and consistently cross-section dependent. Unambiguous that the equivalent geometric imperfection highly depends on the relative slenderness. For ease of application, a constant value of  $L/350$  for equivalent geometric imperfection magnitude is suggested, which is considered safe for all geometries and slenderness analyzed.

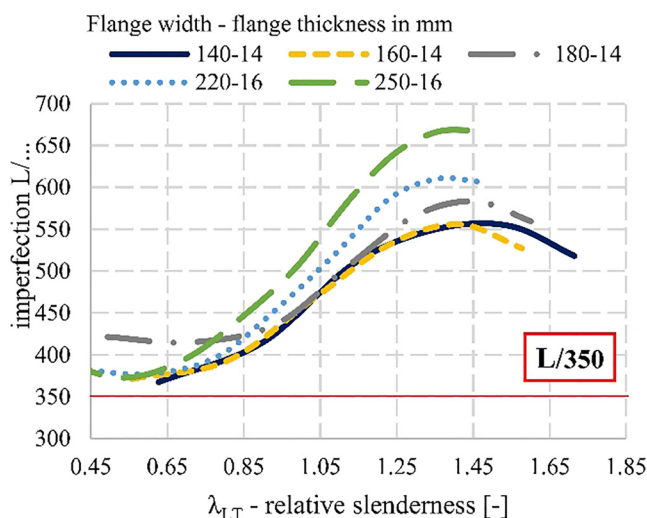


Fig. 3. Effect of varying the flange size on the magnitude of the required equivalent geometric imperfection (Source: Authors' result)

### 3.2. Effect of boundary conditions

In the current parametric study three different support types are used as presented in Section 2.2, namely support #1, when  $k = 1.0$  and  $k_w = 1.0$ ; support #2, when  $k = 1.0$  and  $k_w = 0.5$ ; and support #3, when  $k = 0.5$  and  $k_w = 0.5$ .

The influence of boundary conditions on the elastic critical moment is presented in Fig. 4. In this figure the calculated elastic critical moment is plotted as a function of the span length  $L$ . The elastic critical moment is determined using three methods:

- i) from LBA (i.e., FEM result);
- ii) with the recommendation of Lindner [1]; and
- iii) with the proposal of Lopes et al. [5].

From the results it is clear that the smallest value of elastic critical moment belongs to the support #1 condition, and support #3 has the greatest one as expected from Eq. (1). As the span length increases, the effect of the warping term becomes lower.

The arrangement of support #1 and support #2 converges more quickly and results in the same  $M_{cr}$  for long spans where it is clear that the torsional constant is dominant, and the warping term virtually disappears. Overall, the difference between the two analytical and numerical calculation approaches is not significant, the results obtained with the analytical methods follow well the numerical calculation results.

The numerical results and analytical suggestions are compared. It is observed that Lindner's calculation method

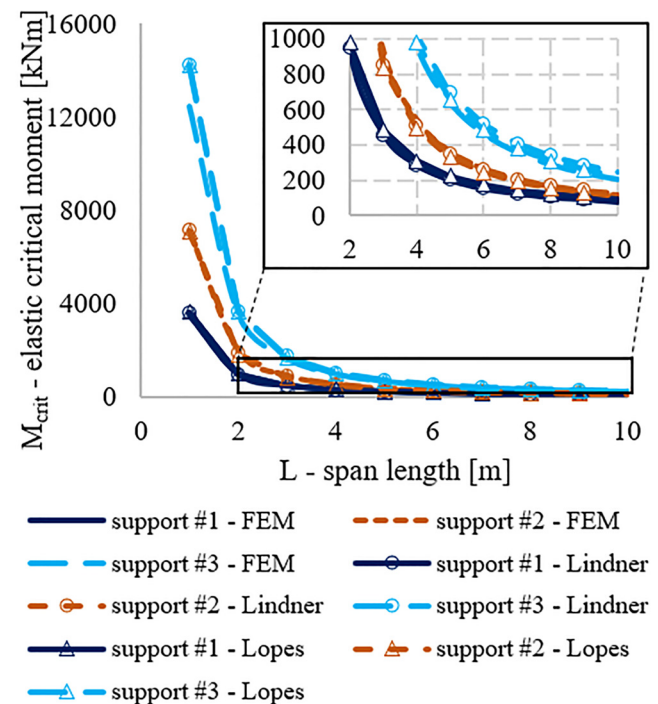


Fig. 4. Influence of boundary conditions on the elastic critical moment using analytical and numerical calculation methods [14] (Source: Authors' result)



is accurate for support #1. When the smallest span is used, comparatively significant differences are observed, which is not surprising since in this case the failure is practically ruled by the strength of the steel. The LBA results also confirm this, as in these tests, not pure lateral-torsion buckling eigenmodes are observed, but eigenmodes combined with local flange buckling.

The influence of boundary conditions on the numerical model-based LTB resistance is also investigated. As expected, the girder has the smallest load-carrying capacity for support #1 since in this case the end sections are free to rotate and warp.

In Fig. 5 the reduction factors obtained using the three types of boundary conditions are presented as a function of relative slenderness. The LTB reduction factors are calculated by Eq. (2) in which  $M_{b,R}$  is the numerical model-based LTB resistance using again  $L/1000$  equivalent geometric imperfection using the scaled-up first global eigenmode shape. The cross-sectional moment capacity is marked by  $M_y$ , which is determined by neglecting the web contribution and by taking into account only the Steiner's terms as given by Eq. (3) following EN 1993-1-5:2006 [15]. In the equation  $b_{f,eff}$  is the effective width given by Jäger et al. [16, 17]. Practically, every data point follows the same curve, independent of the boundary conditions without significant differences. For that reason, in further numerical simulations, only support type #1 is used.

$$\chi_{LT} = \frac{M_{b,R}}{M_y}, \quad (2)$$

$$M_y = b_{f,eff} \cdot t_f \cdot f_{yf} \cdot (h_w + t_f). \quad (3)$$

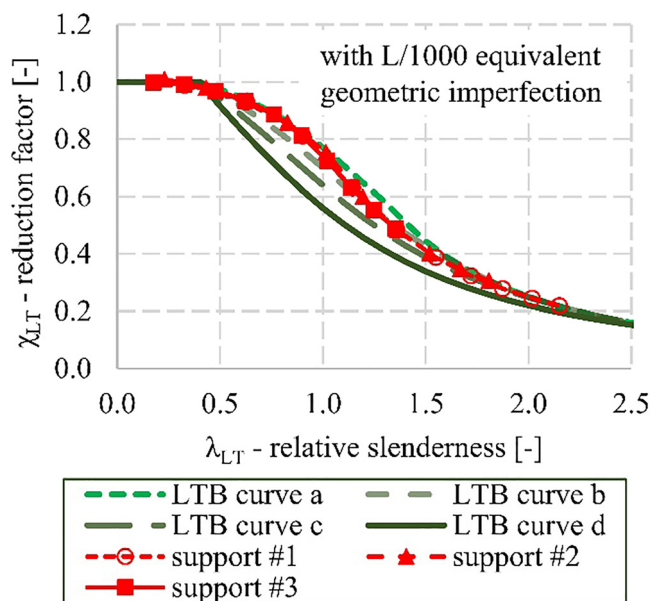


Fig. 5. Effect of support conditions on the reduction factor [14]  
(Source: Authors' result)

### 3.3. Determination of required partial factor

In the deterministic analysis, five cross-sections are tested, in the same way as the imperfection-sensitivity analysis presented in Section 3.1. The applied flange sizes are shown in Table 1. For flange size a), two more different correlation profiles are again investigated as well. The geometric imperfection's magnitude is  $L/1000$  and residual stress is also considered. The numerical results obtained by the deterministic analysis are compared with the flexural buckling curves "a" and "b" and lateral-torsional buckling curves "c" and "d", which are close to the results. In Fig. 6, the four buckling curves are compared with the reduction factors calculated from the linear buckling analysis and geometrical and material nonlinear imperfect analysis results as shown above.

The resulting  $\gamma_{MI}$  partial factors are summarized in Table 2. Based on the statistical evaluation of the deterministic analysis, the smallest partial factor  $\gamma_{MI}$  is associated with the flexural buckling curve b.

The results of the deterministic analysis are statistically evaluated by the method given in Annex D of EN 1990:2002, Section 8.2, [8], comparing the results with the LTB curves c and d (with the parameters:  $\beta = 0.75$  and  $\lambda LT,0 = 0.4$ ) and the flexural buckling curves a and b from EN 1993-1-1:2005 [7]. The resulting  $\gamma_{MI}$  partial factors are summarized in Table 2. Based on the statistical evaluation of the deterministic analysis, the smallest partial factor  $\gamma_{MI}$  is associated with the flexural buckling curve b. However, it is important to underline that for every of the buckling curves investigated, values between 1.0 and 1.1 are obtained.

## 4. CONCLUSION

In the current study, a numerical parametric analysis is presented using deterministic and stochastic methods. The basic aim is the determination of the equivalent geometrical imperfection and the buckling curve applicable in the case of LTB, which are required according to EN 1993-1-1 for the design of trapezoidally corrugated web girders. Highlighting only the most relevant results, the numerical study presented above leads to the following conclusions:

- In this paper, the required equivalent geometric imperfections are calculated in such a way as to give the same resistance in the numerical model-based calculation as using the initial geometric imperfection ( $L/1000$ ) combined with the corresponding residual stress pattern. Based on the results, a constant lower bound, namely  $L/350$ , as recommended equivalent geometric imperfection is given using the scaled first global eigenmode shape;
- The impact of boundary conditions is tested using three versions, by controlling the warping and rotation of the cross-sections at the end of the girder. The support condition does not have a significant impact on the buckling reduction factor (e.g., buckling curve);



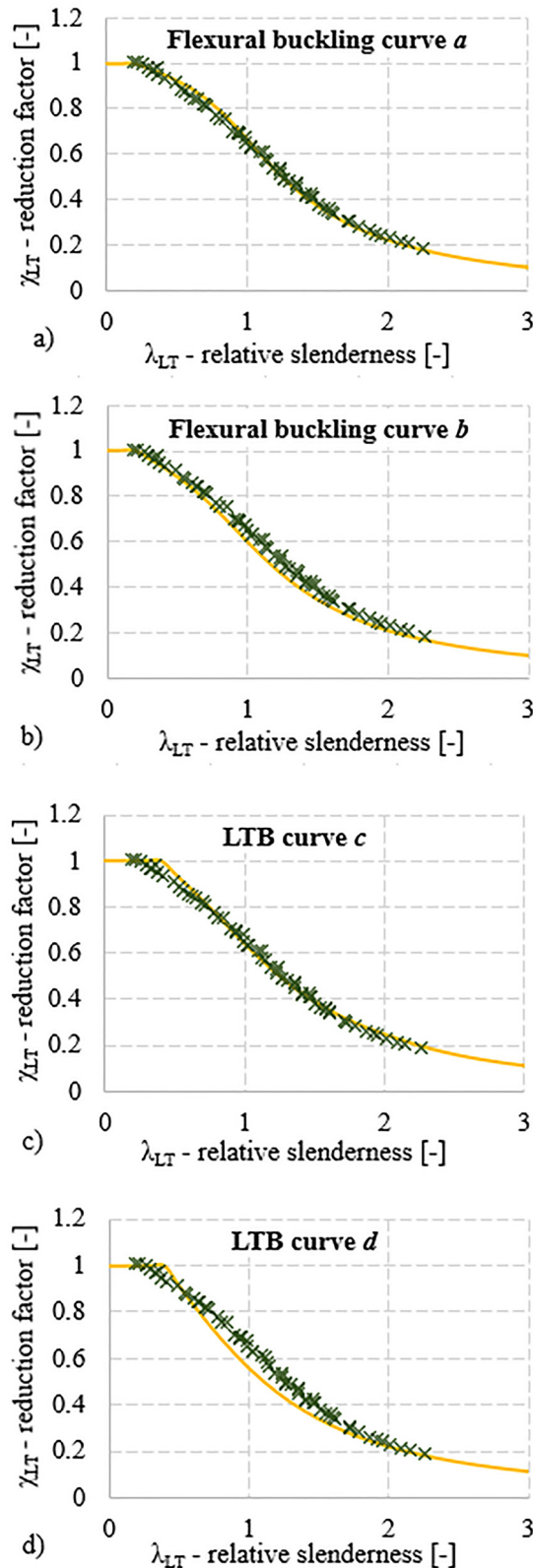


Fig. 6. The reduction factors from the deterministic test and the flexural buckling curves “a” and “b” and the LTB curves “c” and “d” from EN 1993-1-1 [8]

Table 2. Partial factors  $\gamma_{M1}$  determined from the deterministic GMNIA [14]

	$\gamma_{M1}$ [-]
flexural buckling curve a)	1.0562
flexural buckling curve b)	1.0162
LTB curve c)	1.0562
LTB curve d)	1.0753

Source: Authors' result

- From the deterministic analysis it seems that the flexural buckling curve b can be applied for trapezoidally corrugated web girders using partial factor  $\gamma_{M1} = 1.0$ . The other investigated buckling curves (lateral-torsional buckling curves c and d, and flexural buckling curves a) results larger required  $\gamma_{M1}$ ;

## ACKNOWLEDGEMENTS

The research work is connected to the MTA-BME research group “New generation steel bridges” Lendület (LP2021-06/2021) at the BUTE Department of Structural Engineering; the financial support is gratefully acknowledged.

## REFERENCES

- [1] J. Lindner, “Lateral torsional buckling of beams with trapezoidally corrugated webs,” in *Proceedings of the 4th International Colloquium on Stability of Steel Structures*, Budapest, Hungary, April 25–27, 1990, pp. 79–82.
- [2] J. Bartuš and J. Odrobiňák, “Lateral-torsional buckling of nonsymmetrical plate girders with web openings,” *Pollack Period.*, vol. 17, no. 3, pp. 47–52, 2022.
- [3] M. Larsson and J. Persson, “Lateral-torsional Buckling of Steel Girders with Trapezoidally Corrugated Webs,” MSc Thesis, Chalmers University of Technology, Gothenburg, Sweden, 2013.
- [4] V. Ilanovsky, “Assessment of bending moment resistance of girders with corrugated web,” *Pollack Period.*, vol. 10, no. 2, pp. 35–44, 2015.
- [5] G. C. Lopes, C. Couto, P. V. Real, and N. Lopes, “Elastic critical moment of beams with sinusoidal corrugated webs,” *J. Construct. Steel Res.*, vol. 129, pp. 185–194, 2017.
- [6] *EN 1090-2:2018*, Execution of Steel Structures and Aluminum Structures - Part 2: Technical Requirements for Steel Structures, CEN, Brussels, 2018.
- [7] *EN 1993-1-1:2005*, Eurocode 3: Design of Steel Structures - Part 1.1: General Rules and Rules for Buildings, CEN, Brussels, 2005.
- [8] *EN 1990:2002*, Eurocode: Basis of Structural Design, CEN, Brussels, 2002.
- [9] ANSYS® v19.2, Canonsburg, Pennsylvania, USA.
- [10] B. Jáger and L. Dunai, “Nonlinear imperfect analysis of corrugated web beams subjected to lateral-torsional buckling,” *Eng. Struct.*, vol. 245, 2021, Paper no. 112888.

- [11] S. P. Timoshenko and J. M. Gere, *Theory of Elastic Stability*. 2nd ed., McGraw-Hill, London, 1961.
- [12] L. Gardner, X. Yun, A. Fieber, and L. Macorini, "Steel design by advanced analysis: Material modeling and strain limits," *Engineering*, vol. 5, no. 2, pp. 243–249, 2019.
- [13] B. Jáger and L. Dunai, "Nonlinear imperfect analysis of corrugated web beams subjected to lateral-torsional buckling," *Eng. Struct.*, vol. 245, 2021, Paper no. 112888.
- [14] E. Bärnkopf, B. Jáger, and B. Kövesdi, "Lateral-torsional buckling resistance of corrugated web girders based on deterministic and stochastic nonlinear analysis," *Thin-Walled Struct.*, vol. 180, 2022, Paper no. 109880.
- [15] *EN 1993-1-5:2006*, Eurocode 3: Design of Steel Structures Part 1-5: Plated Structural Elements, CEN, Brussels, 2005.
- [16] B. Jáger, L. Dunai, and B. Kövesdi, "Flange buckling behavior of girders with corrugated web, Part I: Experimental study," *Thin-Walled Struct.*, vol. 118, pp. 181–195, 2017.
- [17] B. Jáger, L. Dunai, and B. Kövesdi, "Flange buckling behavior of girders with corrugated web, Part II: Numerical study and design method development," *Thin-Walled Struct.*, vol. 118, pp. 238–252, 2017.

**Open Access.** This is an open-access article distributed under the terms of the Creative Commons Attribution 4.0 International License (<https://creativecommons.org/licenses/by/4.0/>), which permits unrestricted use, distribution, and reproduction in any medium, provided the original author and source are credited, a link to the CC License is provided, and changes - if any - are indicated. (SID\_1)

